


 Cite this: *RSC Adv.*, 2025, **15**, 806

## Preparation and characterization of novel PMMA bone cement containing 3,4-dichloro-5-hydroxyfuran-2(5H)-one†

 Wen-Han Bu,<sup>‡ab</sup> Ayakuzi Asilebieke,<sup>‡d</sup> Lu-Yang Han,<sup>‡ab</sup> Yang Xu,  <sup>\*cd</sup> Tao Zhou<sup>\*c</sup> and Jian-Jun Chu<sup>\*abd</sup>

*Introduction:* to address the issue of burst drug release in antibiotic-loaded poly(methyl methacrylate) (PMMA) bone cement (ALBC), this study involved preparation of novel PMMA bone cement and determination of its antibacterial activity, biocompatibility, compressive properties, maximum temperature, and setting time. *Methods:* a novel acrylic monomer, which contains the 3,4-dichloro-5-hydroxyfuran-2(5H)-one (DHF), was synthesized and utilized to develop non-leaching antibacterial PMMA bone cement (NLBC), designated as DHF-methacrylic acid (DHF-MAA) bone cement. In the preparation of this bone cement, DHF-MAA served as a key component of the liquid phase. Its antibacterial activity was determined using a surface antibacterial assay. The biocompatibility of the cement was evaluated through a rabbit-suspended erythrocyte hemolysis test, assessment of the relative proliferation rate of mouse embryonic osteoblast precursor cells (MC3T3-E1) using the CCK-8 method, and an acute toxicity test in mice. The assessment of compressive properties includes both compressive strength and compressive modulus before and after aging. *Results:* DHF-MAA bone cement exhibited antibacterial activity, excellent biocompatibility, and acceptable compressive properties; in particular, the 10% DHF-MAA bone cement, achieved 100% antibacterial activity, excellent biocompatibility, and a compressive strength that met the compressive value, as stated in ISO 5833. *Conclusions:* in this study, novel antibacterial non-leaching DHF-MAA bone cement was synthesized and evaluated for its antibacterial activity, biocompatibility, and compressive properties. In particular, the 10% DHF-MAA bone cement exhibited excellent antibacterial activity, biocompatibility, and acceptable compressive properties. As such, this cement formulation warrants further characterization with a view to using it to anchor cemented arthroplasties.

Received 13th September 2024

Accepted 4th January 2025

DOI: 10.1039/d4ra06607c

[rsc.li/rsc-advances](http://rsc.li/rsc-advances)

## 1 Introduction

Periprosthetic joint infection (PJI) is one of the most severe complications of arthroplasty, posing a significant threat to patient health and safety.<sup>1,2</sup> To address this challenge, it is common to use an ALBC to anchor the arthroplasty in the prepared bone bed,<sup>3–5</sup> and studies have reported that the

application of ALBC significantly reduces the incidence of PJI.<sup>6,7</sup> However, this method has some problems, such as the burst release of antibiotic(s) in the initial stage, insufficient antibacterial activity in the later stage leading to bacterial resistance to the released antibiotic(s),<sup>8,9</sup> and the degradation of bone cement's mechanical properties due to antibiotic(s) release.<sup>10,11</sup> Thus, there is incentive to develop alternatives to ALBC, with one such alternative being non-leaching PMMA bone cement (NLBC). NLBC combines antibacterial substances with a PMMA skeleton by covalent linkage or physical adsorption, ensuring that the antibacterial substances are not released *in vivo*, but exhibit contact-killing properties.<sup>12,13</sup>

The current generation of NLBC include two major classes of quaternary ammonium compounds and heterocyclic compounds.<sup>14–20</sup> Among them, furanone derivatives, which are heterocyclic compounds, have been widely studied for their good antibacterial activity.<sup>21</sup> Xie modified alumina particles with DHF motifs and found that bone cement that contained these particles possessed good antibacterial activity and satisfactory mechanical properties.<sup>22,23</sup> Fu and Chu *et al.* synthesized

<sup>a</sup>Department of Orthopedics, The Second People's Hospital of Hefei, Hefei Hospital, Affiliated to Anhui Medical University, No. 246 of Heping Road, Yaohai District, Hefei, Anhui 230011, China. E-mail: chujianj@mail.ustc.edu.cn

<sup>b</sup>The Fifth Clinical Medical School of Anhui Medical University, Hefei, Anhui 230032, China

<sup>c</sup>Department of Orthopedics, The People's Hospital of Ma'anshan, Ma'anshan, Anhui 243000, China. E-mail: zty7621@163.com

<sup>d</sup>School of Food and Biological Engineering, Hefei University of Technology, Hefei, Anhui 230009, China. E-mail: xuyang@hfut.edu.cn

† Electronic supplementary information (ESI) available. See DOI: <https://doi.org/10.1039/d4ra06607c>

‡ Wen-Han Bu, Ayakuzi Asilebieke and Lu-Yang Han contributed equally to this work.



an antibacterial monomer, nitro furfuryl methacrylate (NFMA), and copolymerized it with methyl methacrylate (MMA) monomer to make a new type of *p*(NFMA-*co*-MMA) bone cement, which demonstrated increased antibacterial activity compared to PMMA, but with a reduction in compressive properties, with limited research on its biocompatibility.<sup>24</sup> Building on this foundation, Shen and Chu *et al.* extended the side chains of the bone cement to develop long-chain NFMA, which slightly improved the compressive strength and compressive modulus compared to NFMA but still fell short of meeting the requirements for load-bearing bones in the human body.<sup>25</sup> Furthermore, Chu *et al.* identified an *N*-halamine compound that, when incorporated into bone cement, exhibited surface antibacterial effects; however, its poor compressive strength and compressive modulus posed significant limitations for further application.<sup>26</sup>

To the best of our knowledge, the majority of antibacterial motif covalently linked NLBC prepared *via* simple liquid-phase modification do not possess good antibacterial activity, biocompatibility, and mechanical properties simultaneously.<sup>27–29</sup> Our aim was to develop NLBC that excels in all the above-mentioned aspects. For this purpose, we covalently linked DHF with MAA to produce DHF-MAA, an oil-like liquid that is easily soluble in MMA. DHF-MAA was used in the liquid-phase modification of bone cement, ultimately resulting in the preparation of DHF-MAA bone cement. In the present study was to prepare the DHF-MAA bone cement and determine its antibacterial activity, compressive properties, setting time, and biocompatibility.

## 2 Experimental

### 2.1 Materials

PMMA bone cement (OSTEOPAL®V) and ALBC (PALACOS®R+G) were purchased from Heraeus Medical GmbH; DHF was purchased from Guangzhou Ronfan Technology Co., Ltd; MAA from Shanghai Macklin Biochemical Technology Co., Ltd; dichloromethane (DCM), 1-(3-dimethylaminopropyl)-3-ethylcarbodiimide hydrochloride (EDCI), and 4-dimethylaminopyridine (DMAP) were purchased from Shanghai Macklin Biochemical Co., Ltd; *Staphylococcus aureus* (ACTT 25923) was obtained from the Laboratory Department of The Second People's Hospital of Hefei. The other chemicals used were of analytical grade and were used without further purification. C57 mice were purchased from Beijing SPF Biotechnology Co., Ltd.

### 2.2 Synthesis of DHF-MAA monomer

Add DHF (30 mmol, 1.0 eq.) and MAA (36 mmol, 1.2 eq.) to 50 mL of DCM. Then, add EDCI (36 mmol, 1.2 eq.) and DMAP (6 mmol, 0.2 eq.) and stir at room temperature for 3 hours to ensure complete reaction. After the reaction is complete, remove DCM using a rotary evaporator at 40 °C. Dissolve the remaining product in 350 mL of ethyl acetate, and extract using 1 M HCl and 5% sodium carbonate solution. Dry the organic layer with 200 g of anhydrous sodium sulfate. Remove the solvent with a rotary evaporator at 50 °C. Purify the crude product using silica gel column chromatography to obtain the

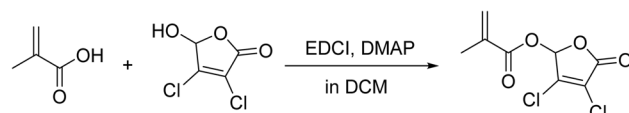


Fig. 1 Synthetic route of DHF-MAA.

final product, DHF-MAA (4.0 g, 16.9 mmol). The preparation steps are shown in Fig. 1. <sup>1</sup>H NMR (400 MHz, CDCl<sub>3</sub>) δ 7.02–6.94 (m, 1H), 6.28 (p, *J* = 0.9 Hz, 1H), 5.88–5.78 (m, 1H), 2.01 (ddd, *J* = 2.6, 1.6, 1.0 Hz, 3H).

### 2.3 Preparation of bone cement specimens

The compositions of the cement formulations used are shown in Table 1. First, DHF-MAA was added to the liquid phase of the bone cement (the concentration of DHF-MAA was calculated as a proportion of its mass in the liquid phase, where it replaced the liquid phase components of OSTEOPAL®V on an equal-mass basis). After thorough shaking, it was mixed with the solid phase of the bone cement and stirred evenly. The mixture was then poured into molds. After hardening, specimens were removed from the mold, thereby to obtain cylindrical bone cement specimens with diameter of 6.0 ± 0.1 mm and a height of 12.0 ± 0.1 mm. These specimens were subjected to compressive strength, compressive modulus and antibacterial activity tests, and the bone cements of each group were soaked with saline according to 5 mL g<sup>-1</sup> and left to stand for 24 h at 37 °C, 5% CO<sub>2</sub> constant temperature incubator to prepare the bone cement extraction solution for biocompatibility evaluation.

### 2.4 Characterization of cement powder

The bone cement powder, which was produced by grinding individual specimens using a metal file, containing DHF-MAA at concentrations of 2.5%, 5%, and 10% was thoroughly mixed with potassium bromide at a ratio of approximately 1 : 50, ground, and pressed into pellets. The prepared specimens were analyzed using an Fourier-transform infrared spectra (FT-IR) spectrometer, and spectra were recorded on a BRUKER VECTOR-22 spectrometer over a frequency range of 4000–400 cm<sup>-1</sup>. The FT-IR were plotted using Origin software.

### 2.5 Determination of antibacterial activity

**2.5.1 Contact antibacterial experiment.** *Staphylococcus aureus* (ACTT 25923) was revived and subcultured to restore its viability. Bone cement specimens were synthesized the day before the experiment and soaked in 3 mL of distilled water for 18 h to remove any unpolymerized DHF-MAA monomers on the surface. On the day of the experiment, a bacterial suspension with a concentration of (0.5 × 10<sup>8</sup>) CFU mL<sup>-1</sup> was prepared. Each bone cement specimen was soaked in 1 mL of the bacterial suspension and incubated at 37 °C in a CO<sub>2</sub> incubator for 6 hours. The specimens were then removed and gently rinsed with 100 mL of distilled water to remove non-adherent bacteria. The specimens were placed in 5 mL of saline and sonicated for

Table 1 Formulation of PMMA cement and various concentrations of DHF-MAA bone cement (percentage by mass of each component)

Formulation	Powder (%)			Liquid (%)		
	PMMA	ZrO <sub>2</sub>	BPO	MMA	DMPT	DHF-MAA
PMMA cement	34.83	28.71	0.24	35.43	0.77	0
2.5% DHF-MAA cement	34.83	28.71	0.24	34.54	0.75	0.91
5% DHF-MAA cement	34.83	28.71	0.24	33.66	0.73	1.81
7.5% DHF-MAA cement	34.83	28.71	0.24	32.77	0.71	2.72
10% DHF-MAA cement	34.83	28.71	0.24	31.89	0.69	3.62

3 min to dislodge adherent bacteria. Then, the specimen was removed and the remaining liquid was retained, from which 40  $\mu$ L was aspirated and diluted 100-fold, mixed thoroughly, and then 40  $\mu$ L was taken from the diluted bacterial solution and spread evenly in the Petri dish. The Petri dishes were incubated at 37 °C in a CO<sub>2</sub> incubator for 1 day, after which colony counts were performed to calculate the surface antibacterial index of the specimen. Each concentration of bone cement was tested in five replicates.

$$\text{Index of antibacterial activity} = \frac{A - B}{A} \times 100\% \quad (1)$$

In the above equation,  $A$  represents the number of colonies on the Petri dishes with the PMMA cement group, while  $B$  represents the number of colonies on the Petri dishes with different concentrations of DHF-MAA bone cement group.

**2.5.2 Leaching test.** To test whether DHF-MAA bone cement exhibits leaching, we prepared five specimens each of PMMA bone cement, 10% DHF-MAA bone cement, and ALBC (containing 1.25% gentamicin sulfate, the formula for ALBC is shown in Table S1†). Each specimen was placed in 3 mL of saline solution, sealed, and left to stand at 37 °C for 1 day. Subsequently, 1 mL of saline and 1 mL of extract from each group were mixed with a *Staphylococcus aureus* suspension containing ( $0.5 \times 10^8$ ) CFU mL<sup>-1</sup> and incubated at 37 °C in a CO<sub>2</sub> incubator for 6 hours. The bacterial solutions were then diluted 2500-fold, and 40  $\mu$ L of the diluted solution was evenly spread onto Petri dishes. The Petri dishes were incubated at 37 °C in a CO<sub>2</sub> incubator for another day to allow for bacterial colony counting. Colony numbers in the saline control group were compared with those in the extract groups.

## 2.6 *In vitro* biocompatibility

**2.6.1 Hemolysis test.** Preparation of 2% rabbit red blood cell suspension: collect arterial blood from male New Zealand rabbits and centrifuge it (1000 rpm, 15 min) in tubes to remove the plasma and other fluids. Resuspend the precipitated red blood cells in saline and centrifuge again to remove the supernatant for higher purity. Finally, add saline to prepare a 2% rabbit red blood cell suspension and store it at 4 °C.

Experimental procedure: first, soak a bone cement specimen in 3 mL of saline for 1 hour. Then, mix each extract with a 2% rabbit red blood cell suspension at a 9 : 1 ratio and incubate at 37 °C in an electromagnetic incubator for 1 hour. Finally,

centrifuge the mixture (3000 rpm, 5 min) and measure the optical density (OD) of the supernatant using a spectrophotometer (Nanodrop One). Simultaneously, measure the OD values of the negative control group (saline) and the positive control group (distilled water) mixed in the same ratio to calculate the hemolysis index of the bone cement extracts in each group.

$$\text{Hemolysis index} = \frac{\text{OD}_T - \text{OD}_N}{\text{OD}_P - \text{OD}_N} \times 100\% \quad (2)$$

In the above equation, OD<sub>T</sub> is the OD of the experimental group, OD<sub>N</sub> is the OD of the negative control group (saline), and OD<sub>P</sub> is the OD of the positive control group (distilled water).

### 2.6.2 *In vitro* cell proliferation and toxicity experiments.

MC3T3-E1 cells were seeded into 96-well plates at a density of 4000 cells per well, using DMEM/F12 medium containing 10% fetal bovine serum and 1% double antibiotics. Incubate at 37 °C in a saturated humidity environment with 5% CO<sub>2</sub>. After the cells adhere, add an extract of bone cement extract and perform a CCK-8 assay. Add CCK-8 at 1/10 of the well volume and continue incubation for 4 hours. Measure the OD at 450 nm using a microplate reader to calculate the relative growth rate (RGR) of the cells. Similarly, measure the OD on days 1, 3, and 5 and calculate the RGR. Evaluate the changes in cell morphology and cytotoxicity according to GB/T 16886 standards.

$$\text{RGR} = \frac{\text{OD}_{T'} - \text{OD}_R}{\text{OD}_{N'} - \text{OD}_R} \times 100\% \quad (3)$$

In the above equation, OD<sub>T'</sub> is the OD of the experimental group, OD<sub>N'</sub> is the OD of the control group (complete medium), and OD<sub>R</sub> is the OD of the cell-free medium.

## 2.7 Determination of compressive properties

The cylindrical bone cement specimens (5 per group) were ground with 1000-grit sandpaper until the top and bottom surfaces were parallel. The specimens were incubated at 37 °C and 100% humidity for 24 hours. The specimens were incubated at 37 °C and 100% humidity for 24 hours to facilitate determination of compressive properties. For aged cement specimens of compressive properties, the specimens were soaked in 10 mL of physiological saline at 37 °C in a CO<sub>2</sub> incubator for 14 days. At room temperature, the deformation-load curves of the bone cement specimens were plotted using



a computer-controlled materials testing machine (MTS809, Bose Corporation, USA) with a crosshead displacement rate of  $20 \text{ mm min}^{-1}$ . The compressive strength and compressive modulus of each bone cement specimen were calculated from these curves. All operations were performed in accordance with the requirements and standards of ISO 5833.

## 2.8 Setting time test

Conduct experiments under the conditions of  $24 \pm 1 \text{ }^{\circ}\text{C}$  with a relative humidity of  $40 \pm 5\%$ . Record the ambient temperature ( $T_{\text{amb}}$ ). Fill 1 g of well-mixed bone cement into a mold designed for polymerization temperature measurement and use an infrared thermography camera to record the changes in temperature over time during the polymerization process. Note the maximum temperature ( $T_{\text{max}}$ ). The setting temperature ( $T_{\text{set}}$ ) is calculated using the formula  $T_{\text{set}} = (T_{\text{max}} + T_{\text{amb}})/2$ . The setting time ( $t_{\text{set}}$ ) corresponds to the time when  $T_{\text{set}}$  is reached. Test three specimens each of PMMA cement and DHF-MAA bone cement at various concentrations under the same experimental conditions, and calculate the average values.

## 2.9 Acute toxicity test in mice

Thirty 8 week-old male C57 mice were prepared and assigned randomly to 6 groups of 5 mice each. The experimental group (extract of a bone cement) and the control group (saline group) were injected into the peritoneal cavity of the mice at a dose of  $50 \text{ mL kg}^{-1}$ , respectively, and then, the mice were sacrificed after 3 days under the feeding conditions of room temperature and sufficient food. The livers and kidneys of the mice were fixed with formalin solution for 1 day before dehydrating them using ethanol, fixing them in sealing wax, drying the slices, and then staining their liver and kidney sections using Hematoxylin–Eosin staining. The purpose of work was to observe the liver and kidney sections and to determine whether the DHF-MAA bone cement extraction solution caused acute toxic reactions in the mice according to GB/T 16886.

## 2.10 Statistical analysis

Quantitative results were expressed as mean  $\pm$  standard deviation. The antibacterial index, hemolysis index, compressive properties, maximum temperature, setting time and RGR (at the same time points) results were analyzed using non-parametric Kruskal–Wallis test, followed by pairwise comparisons adjusted with the Bonferroni correction method. The Friedman rank test was used to analyze the relative cell proliferation rates at different time points within the same group, as well as the compressive strength and compressive modulus results before and after aging. All these analyses were performed using a commercially-available software package (SPSS Statistics, Version 27; IBM, Inc., Armonk, New York, USA).

## 3 Results and discussion

The FT-IR results of PMMA cement and 2.5%, 5%, and 10% DHF-MAA bone cement are shown in Fig. 2. In addition to exhibiting the same characteristic peaks as PMMA bone cement

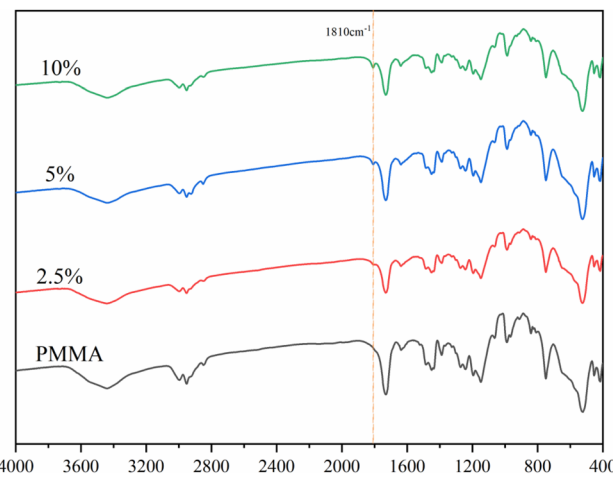


Fig. 2 FT-IR spectra of the powder of PMMA cement and three DHF-MAA bone cement formulations.

at  $2952 \text{ cm}^{-1}$ ,  $1730 \text{ cm}^{-1}$ ,  $1242 \text{ cm}^{-1}$ , and  $1154 \text{ cm}^{-1}$ , the DHF-MAA bone cement also showed a new characteristic peak at  $1810 \text{ cm}^{-1}$  due to pseudo ester formation. The intensity of this peak increased with the amount of DHF-MAA added, indicating that more DHF-MAA was polymerized into the PMMA bone cement.

The results (Fig. 3B) indicate that the addition of DHF-MAA has a significant impact on the index of antibacterial activity of DHF-MAA bone cement, with statistically significant differences ( $p < 0.001$ ). Among them, the index of antibacterial activity of 10% DHF-MAA bone cement shows significant differences compared to 2.5% DHF-MAA bone cement ( $p < 0.001$ ) and 5% DHF-MAA bone cement ( $p < 0.05$ ). During the experiment, colonies of *Staphylococcus aureus* of varying sizes were observed on the Petri dishes that contained 2.5%, 5%, and 7.5% DHF-MAA bone cement specimens (Fig. 3A), indicating that some

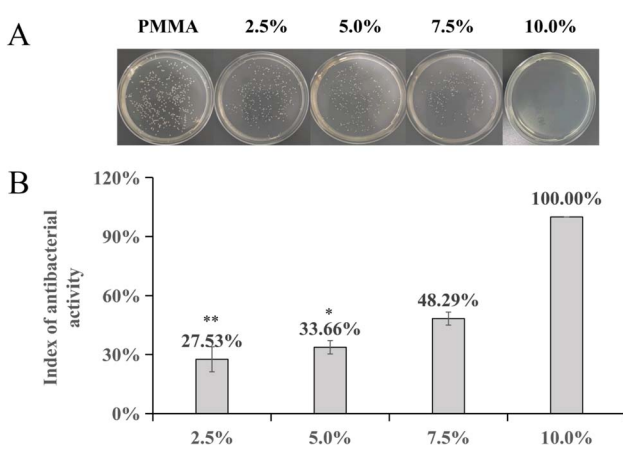


Fig. 3 (A) Petri dishes containing extracts from specimens of PMMA cement and four DHF-MAA bone cement formulations; (B) bar charts of the antibacterial indexes of DHF-MAA bone cement formulations. (\* indicates  $p < 0.05$  compared to the 10% DHF-MAA bone cement group, \*\* indicates  $p < 0.001$  compared to the 10% DHF-MAA bone cement group).



bacterial growth occurred. When the concentration reached 10%, no bacterial growth was observed in the Petri dish, achieving a 100% index of antibacterial activity. This may be related to the antibacterial mechanism of DHF. DHF-MAA cement relies on a contact-kill antibacterial mechanism. The results of the leaching test indicate that compared to the NS (normal saline) group, the extract of DHF-MAA cement did not demonstrate antibacterial activity, similar to PMMA cement ( $p > 0.05$ ). In contrast, the ALBC exhibited a significant difference ( $p < 0.05$ ) (Table S2<sup>†</sup>). Currently, the exact antibacterial mechanism of DHF is not fully understood, but it may include the following aspects: furanone compounds interfere with bacterial quorum sensing systems, inhibiting their communication signal molecules, thereby preventing biofilm formation. Alternatively, DHF can induce the generation of reactive oxygen species, causing oxidative damage to bacterial intracellular proteins and DNA, ultimately leading to cell death.<sup>30</sup> Therefore, specimens of low concentrations of DHF-MAA bone cement allowed some bacterial growth, but high concentrations showed complete antibacterial performance.

After conducting hemolysis tests on DHF-MAA bone cement extracts of different concentrations, visual inspection showed no obvious hemolysis (Fig. 4A). The OD values of the centrifuged supernatants were further measured using a spectrophotometer (Nanodrop One), and the hemolysis indexes were calculated based on the results (Fig. 4B). The experiments demonstrated that the hemolysis indexes of DHF-MAA bone cement extracts at all concentrations were  $<5\%$ , with DHF-MAA producing no statistically significant differences in hemolysis indexes ( $p > 0.05$ ). Therefore, the test results showed that DHF-MAA bone cement does not cause hemolysis of rabbit red blood cells.

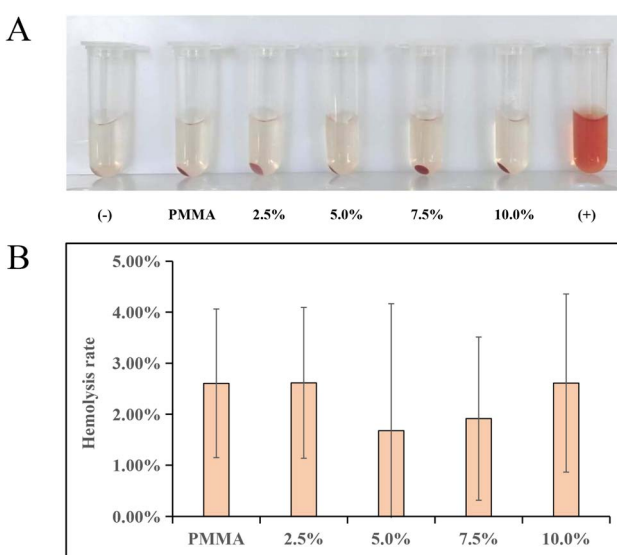


Fig. 4 (A) Visual inspection of hemolysis test results for the PMMA cement and four DHF-MAA bone cement formulations; negative control group (−); and positive control group (+); (B) bar chart of hemolysis indexes for the PMMA cement group and four DHF-MAA bone cement formulations.

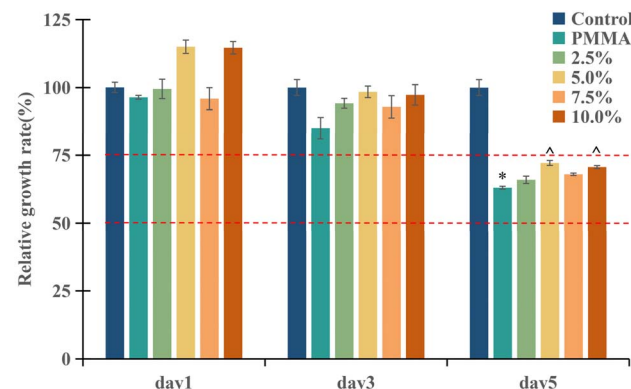


Fig. 5 Bar charts of RGR for the control group (complete medium), PMMA cement group and four DHF-MAA bone cement formulations day 1, day 3, and day 5. (\* indicates  $p < 0.05$  compared to the control group, and ^ indicates  $p < 0.05$  when compared to the same concentration on day 1).

The results of the relative cell proliferation rate of different concentrations of DHF-MAA bone cement measured by the CCK-8 method are shown in Fig. 5. According to the analysis based on GB/T 16886 standards, the relative cell proliferation rate of bone cement at each concentration increased on the 1st and 3rd days, and all were  $>75\%$ , indicating showing no cytotoxicity. On the 5th day, the RGR of both the PMMA cement group and the DHF-MAA bone cement groups at various concentrations were between 50% and 75%, indicating mild cytotoxicity.<sup>31</sup> On the first and third days of the experiment, there were no notable differences in RGR among the various groups ( $p > 0.05$ ). However, on the fifth day, the PMMA cement group exhibited a decrease in RGR compared to the control group ( $p < 0.05$ ). Furthermore, the RGR of the PMMA cement, 5% DHF-MAA bone cement, and 10% DHF-MAA bone cement all declined on the fifth day compared to the first day ( $p < 0.05$ ). For the remaining groups, no statistical differences were observed in RGR when comparing across the three days ( $p > 0.05$ ). It has been stated that various constituents of a PMMA bone cement may adversely affect its biocompatibility.<sup>32,33</sup> Therefore, the mild cytotoxicity observed in groups other than the control group may be due to the contrast agent added to the bone cement (e.g.,  $ZrO_2$  in the bone cement used in this experiment) not participating in the polymerization reaction, leading to incomplete polymerization of some MMA monomers and resulting in some level of cytotoxicity.<sup>34</sup>

The compressive properties results are shown in Fig. 6 from which it is seen that each cement met the requirements of ISO 5833. In compressive strength tests, only the 7.5% and 10% DHF-MAA bone cement exhibited significant reductions in compressive strength compared to the PMMA cement ( $p < 0.05$ ). In the comparison of compressive strength before and after aging for bone cement with the same concentration, the 7.5% DHF-MAA bone cement showed an increase ( $p < 0.05$ ). In compressive strength tests of aged cements, there were no statistically significant differences among the groups ( $p > 0.05$ ). In compressive modulus tests, there were no statistically



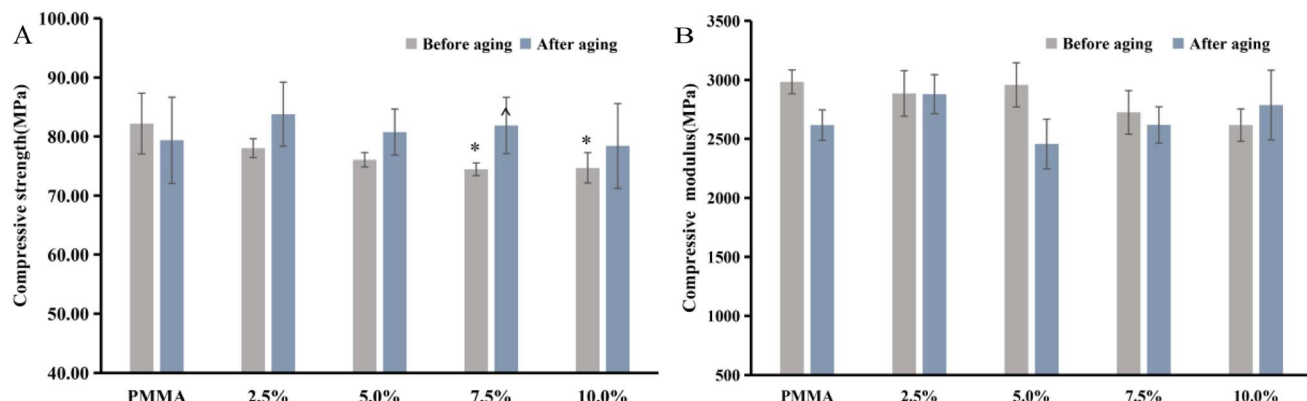


Fig. 6 Compressive strength (A) and compressive modulus (B) of PMMA cement and three four DHF-MAA bone cement formulations. (\* indicates  $p < 0.05$  compared to the PMMA group, ^ indicates  $p < 0.05$  when compared to the same group before aging.)

significant differences among the groups ( $p > 0.05$ ). The compressive strength of bone cement with 7.5% and 10% DHF-MAA showed inconsistencies before and after aging, potentially due to errors arising from the small specimen size. Therefore,

we believe that the addition of DHF-MAA in bone cement may not significantly affect the compressive strength and compressive modulus. Furthermore, the compressive strength of each of the cement formulations was acceptable in that it was  $>70$  MPa.

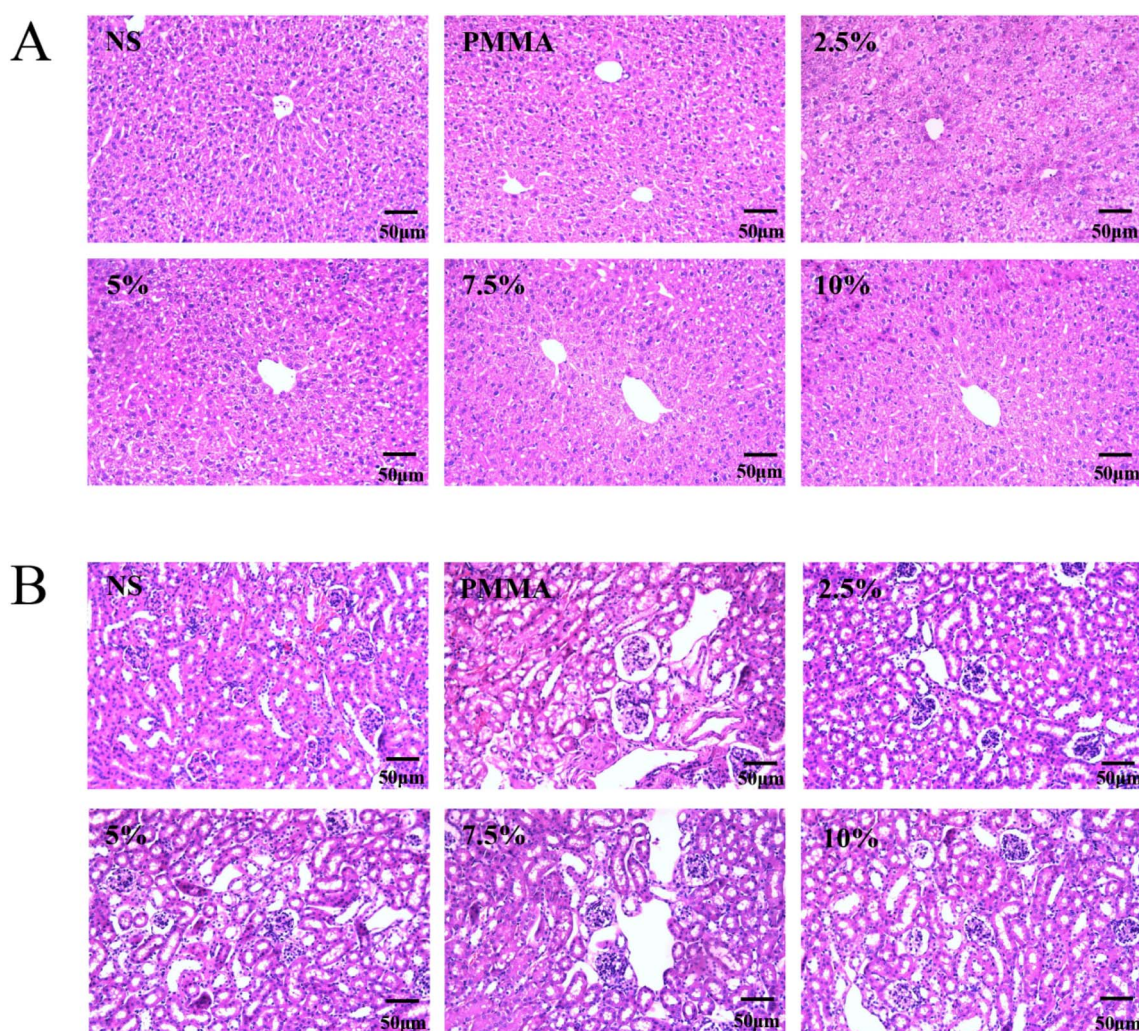


Fig. 7 Slices of liver (A) and kidney (B) of mice from the normal saline (NS) group, PMMA cement group, and the DHF-MAA bone cement groups.



The test results for the maximum temperature and setting time of bone cement are shown in Table S3.† The maximum temperature of 10% DHF-MAA bone cement decreased compared to that of 2.5% DHF-MAA bone cement ( $p < 0.05$ ). Additionally, it exhibited an extended setting time compared to PMMA cement. There were no statistical differences among the other groups ( $p > 0.05$ ). The 10% DHF-MAA bone cement group exhibits a decrease in maximum temperature and an extension of the setting time. This phenomenon may be attributed to the larger molecular weight of DHF-MAA, reducing the mole amount of olefins available for polymerization, and the proportional replacement of the original liquid phase components in OSTEOPAL®V with DHF-MAA, resulting in a corresponding decrease in DMPT content (as shown in Table 1).

In the acute toxicity test conducted on mice, no coma, shock, vomiting, diarrhea, or any other symptoms were observed in any of the mice following the injection of the extract. The liver and kidney sections of mice in each group are shown in Fig. 7. Compared with the saline group, the normal structure of the liver lobules and glomeruli was not damaged by the extract of any of the cement formulations, and no inflammatory cells and necrotic liver and kidney cells were found in the field of view. Therefore, the test results show that DHF-MAA bone cement does not induce acute toxicity reactions in mice.

This study has basically confirmed that DHF-MAA bone cement is a novel NLBC with good antibacterial activity, achieving 100% antibacterial activity at a concentration of 10%. Compared to previously reported NLBCs, while the addition of high concentrations of DHF-MAA does lead to a reduction in compressive strength, it is noteworthy that its compressive strength still meets the ISO 5833 standard. Additionally, the compressive strength of DHF-MAA bone cement is comparable to that of PMMA cement, which is an attribute not achieved by most other NLBCs. Although DHF-MAA bone cement exhibited mild cytotoxicity, it did not increase with higher concentrations, which also differentiates it from other NLBCs.

This study still has certain limitations. During the antibacterial performance testing, we also attempted to evaluate the antibacterial effect of DHF-MAA bone cement against *Escherichia coli*, but regrettably, we found that it lacked antibacterial activity against this bacterium. Additionally, the long-term antibacterial properties and anti-biofilm formation capabilities of DHF-MAA bone cement have not been studied. Therefore, further research is needed to determine whether DHF-MAA bone cement can effectively prevent PJI. Furthermore, the reasons for the inconsistent compressive strength of DHF-MAA bone cement before and after aging have not been fully elucidated, and a reasonable explanation may be found at the microscopic level. Moreover, long-term biocompatibility has not been tested. Therefore, this study merely establishes the first step in exploring the potential clinical application of DHF-MAA bone cement in joint replacement surgery.

## 4 Conclusions

We synthesized a novel antibacterial monomer called DHF-MAA and used a liquid-phase modification strategy to prepare a new

antibacterial NLBC, named DHF-MAA bone cement. This bone cement exhibited excellent antibacterial performance and biocompatibility and acceptable compressive strength. Notably, the 10% DHF-MAA bone cement demonstrated 100% antibacterial activity, excellent biocompatibility, and acceptable compressive strength. Thus, this bone cement deserves further study to establish its suitability for use in anchoring arthroplasties.

## Ethics statement

The animal study was approved by this study was conducted with approval from the Biomedical Ethics Committee of Hefei University of Technology (No. HFUT20220522-001) and complied with the National Institutes of Health Guide for the Care and Use of Laboratory Animals. This study was conducted in accordance with the declaration of Helsinki. The study was conducted in accordance with the local legislation and institutional requirements.

## Data availability

The data used to support the findings of this study are available from the corresponding author upon request.

## Author contributions

Conception and design of the research: Jian-Jun Chu, Yang Xu. Acquisition of data: Wen-Han Bu, Lu-Yang Han, Ayakuzi Asilebieke. Analysis and interpretation of the data: Wen-Han Bu, Lu-Yang Han, Yang Xu. Statistical analysis: Wen-Han Bu, Lu-Yang Han, Yang Xu. Obtaining financing: Jian-Jun Chu, Yang Xu. Writing of the manuscript: Wen-Han Bu, Yang Xu. Critical revision of the manuscript for intellectual content: Jian-Jun Chu, Yang Xu, Tao Zhou.

## Conflicts of interest

The authors declare that the research was conducted in the absence of any commercial or financial relationships that could be construed as a potential conflict of interest.

## Acknowledgements

The authors gratefully acknowledge the Health research Project of Anhui Province (AHWJ2022b091), Hefei Municipal Health Commission Applied Medical Project (HwK2023zd011), the financial support from the Anhui Provincial Natural Science Foundation (2308085QB47), the Fundamental Research Funds for the Central Universities (JZ2023HGQA0114).

## References

- 1 P. Sendi, P. O. Löttscher, B. Kessler, P. Graber, W. Zimmerli and M. Clauss, *Bone Jt. J.*, 2017, **99**, 330–336.
- 2 L. Knoll, S. D. Steppacher, H. Furrer, M. C. Thurnheer-Zürcher and N. Renz, *Bone Jt. J.*, 2023, **105**, 1294–1302.



3 E. L. Cyphert, G. D. Learn, D. W. Marques, C. Y. Lu and H. A. von Recum, *ACS Biomater. Sci. Eng.*, 2020, **6**, 4024–4035.

4 E. L. Cyphert, C. Y. Lu, D. W. Marques, G. D. Learn and H. A. Von Recum, *Biomacromolecules*, 2020, **21**, 854–866.

5 A. E. Levack, K. Turajane, X. Yang, A. O. Miller, A. V. Carli, M. P. Bostrom and D. S. Wellman, *J. Bone Jt. Surg.*, 2021, **103**, 1694–1704.

6 S. S. Jameson, A. Asaad, M. Diamant, A. Kasim, T. Bigirumurame, P. Baker, J. Mason, P. Partington and M. Reed, *Bone Jt. J.*, 2019, **101**, 1331–1347.

7 J. W. Leong, M. J. Cook, T. W. O'Neill and T. N. Board, *Bone Jt. J.*, 2020, **102**, 997–1002.

8 L. H. Cobb, E. M. McCabe and L. B. Priddy, *J. Orthop. Res.*, 2020, **38**, 2091–2103.

9 Y. Al Thaher, S. Perni and P. Prokopovich, *Adv. Colloid Interface Sci.*, 2017, **249**, 234–247.

10 S. P. von Hertzberg-Boelch, M. Luedemann, M. Rudert and A. F. Steinert, *Biomedicines*, 2022, **10**, 1830.

11 Y. Xu, H. Lin, Z. Gao, R. Guo, Y. C. Kan, L. Y. Han, W. H. Bu, Z. Wang, A. Asilebrieke, L. X. Han, C. Li, F. He and J. J. Chu, *J. Mater. Chem. B*, 2024, **12**, 4389–4397.

12 G. Wang, W. Jiang, S. Mo, L. Xie, Q. Liao, L. Hu, Q. Ruan, K. Tang, B. Mehrjou, M. Liu, L. Tong, H. Wang, J. Zhuang, G. Wu and P. K. Chu, *Adv. Sci.*, 2020, **7**, 1902089.

13 H. Lin, Z. Gao, T. Shan, A. Asilebrieke, R. Guo, Y. C. Kan, C. Li, Y. Xu and J. J. Chu, *J. Orthop. Surg. Res.*, 2024, **19**, 673.

14 S. Deb, R. Doiron, L. Disilvio, S. Punyani and H. Singh, *J. Biomed. Mater. Res. B*, 2008, **85**, 130–139.

15 C. K. Abid, S. Jain, R. Jackeray, S. Chattopadhyay and H. Singh, *J. Biomed. Mater. Res. B*, 2017, **105**, 521–530.

16 W. Zhu, F. Liu and J. He, *J. Mech. Behav. Biomed. Mater.*, 2017, **74**, 176–182.

17 X. Sun, Z. Qian, L. Luo, Q. Yuan, X. Guo, L. Tao, Y. Wei and X. Wang, *ACS Appl. Mater. Interfaces*, 2016, **8**, 28522–28528.

18 Z. Gao, Y. C. Kan, Y. H. Xie, R. Guo, C. Li, A. Asilebrieke, Y. Xu and J. J. Chu, *AIP Adv.*, 2023, **13**, 105034.

19 S. Punyani, S. Deb and H. Singh, *J. Biomater. Sci., Polym. Ed.*, 2007, 131–145.

20 X. Sun, Z. Qian, L. Luo, Q. Yuan, X. Guo, L. Tao, Y. Wei and X. Wang, *ACS Appl. Mater. Interfaces*, 2016, **8**, 28522–28528.

21 P. Zhang, W. Chen, Y. C. Ma, B. Bai, G. Sun, S. Zhang, X. Chang, Y. Wang, N. Jiang, X. Zhang and S. Ma, *J. Med. Chem.*, 2023, **66**, 8441–8463.

22 Y. Chen, G. Caneli, R. Almousa and D. Xie, *J. Mech. Behav. Biomed. Mater.*, 2022, **129**, 105135.

23 Y. Chen, G. Caneli and D. Xie, *J. Biomater. Sci., Polym. Ed.*, 2022, 1398–1414.

24 J. Chu, C. Li, J. Guo, Y. Xu and Y. Fu, *Polym. Chem.*, 2022, **13**, 4675–4683.

25 H. Lin, Z. Gao, L.-Y. Han, J.-J. Chu, Y. Xu and D.-H. Shen, *Front. Mater.*, 2024, **11**, 1432482.

26 R. Guo, Y. C. Kan, Y. Xu, L. Y. Han, W. H. Bu, L. X. Han, Y. Y. Qi and J. J. Chu, *Front. Bioeng. Biotechnol.*, 2024, **12**, 1414005.

27 H. Wang, T. Maeda and T. Miyazaki, *J. Biomater. Appl.*, 2021, **36**, 311–320.

28 W. Zhu, C. Lao, S. Luo, F. Liu, Q. Huang, J. He and Z. Lin, *J. Biomater. Sci., Polym. Ed.*, 2018, 635–645.

29 H. Shi, Q. Zhuang, A. Zheng, P. Zhan, Y. Guan, D. Wei, X. Xu and T. Wu, *Chem. Biodiversity*, 2022, **19**, e202100753.

30 I. S. Sharafutdinov, A. S. Pavlova, F. S. Akhatova, A. M. Khabibrakhmanova, E. V. Rozhina, Y. J. Romanova, R. Fakhrullin, O. A. Lodochnikova, A. R. Kurbangalieva, M. I. Bogachev and A. R. Kayumov, *Int. J. Mol. Sci.*, 2019, **20**, 694.

31 State Administration for Market Regulation of China, *Biological Evaluation of Medical Devices: GB/T 16886-2021*, Standards Press of China, Beijing, 2022, pp. , pp. 6–11.

32 Z. Gao, Y. Xu, Y. Kan, H. Li, R. Guo, L. Han, W. Bu and J. Chu, *J. Orthop. Surg. Res.*, 2023, **18**, 569.

33 Y. C. Kan, R. Guo, Y. Xu, L. Y. Han, W. H. Bu, L. X. Han and J. J. Chu, *J. Orthop. Surg. Res.*, 2024, **19**, 169.

34 P. Lopes, M. P. Garcia, M. H. Fernandes and M. H. Fernandes, *J. Biomater. Appl.*, 2013, **28**, 498–513.

